Long-Range Surface Reconstruction: Si(110)-(16 × 2)

A. A. Stekolnikov, J. Furthmüller, and F. Bechstedt

Institut für Festkörpertheorie und -optik, Friedrich-Schiller-Universität, 07743 Jena, Germany

(Received 14 April 2004; published 22 September 2004)

A variety of reconstruction models is studied for the Si(110)-(16 × 2) surface using first-principles calculations. Assuming appropriate rebonding of edge atoms and surface chains buckled in antiphase, we show that steps along the $[\bar{1}12]$ direction yielding a trench indeed lower the surface energy. We explain the long-range surface reconstruction and develop a geometry model based on steps, adatoms, tetramers, and interstitials. The model is able to explain the stripes of paired pentagons seen obviously in empty-state scanning tunneling microscopy images.

DOI: 10.1103/PhysRevLett.93.136104 PACS numbers: 68.35.Bs, 68.35.Md, 68.37.Ef, 73.20.At

Low-index surfaces of group-IV semiconductors such as Si(111)-(7 × 7) or Ge(111)c(2 × 8) show long-range reconstructions. This tendency is also observable in the (110) case. Nonvicinal, clean, and well-annealed Si(110) surfaces exhibit a 16 × 2 reconstruction [1], the atomic structure of which is still unknown. In recent years important structural details have been obtained from scanning tunneling microscopy (STM) experiments [1–5]. They clearly showed that the bond rotation and bond contraction relaxation accompanied with zigzag chains along the $[\bar{1}10]$ direction, i.e., the mechanism on the (110)1 × 1 surfaces of III–V semiconductors, does not occur in the Si(110) case. Rather, STM studies [1–5] suggested that a 16 × 2 reconstructed Si(110) surface consists of equally spaced and alternately raised (up-stripes) and lowered (down-stripes) stripes parallel to the $[\bar{1}12]$ direction which are separated by atomic steps with height $a_0/2\sqrt{2}$ (a_0 is the bulk lattice constant).

The STM images of the stripes are less clear and consequently led to different local pictures and atomic structures [1,4,5]. This concerns the contradictory results obtained for filled-state and empty-state images, the clarity of the images, as well as the spot arrangements. In any case, the stripes consist of zigzag pattern with a repetition distance of $\sqrt{6}a_0$ [5]. The stripes are stacks of paired elements whose shape is interpreted differently by the various authors: octets [6], pentagons [4], or even arrangements of centered stretched hexagons [5]. Based on the different numbers of observed spots, several atomic geometries have been proposed to interpret the Si(110)-(16 × 2) surface including different reconstruction elements, e.g., adatoms, dimers, missing rows, and tetramers with interstitial atoms [1,4,5,7,8]. However, there are no total-energy calculations for the resulting structures, only for isolated structural elements and smaller unit cells [9–12].

In order to understand the atomic geometry and the bonding of the Si(110)-(16 × 2) surface, one has to study the energetic preference and the structure of the step configuration observed by STM. Until now there has been no idea why steps may occur on a flat, nonvicinal low-index surface and how they contribute to the stabilization of the 16 × 2 translational symmetry. First-principles calculations exist only for the Ge(110)-(16 × 2) surface [13]. They suggest a higher surface energy when steps are introduced, in contrast to the experimental observations of images in form of stripes on lower and higher terraces also for germanium [14].

In this Letter we present results of a systematic study of the 16 × 2 reconstruction of the Si(110) surface based on *ab initio* calculations. Whole 16 × 2 unit cells with nominally 64 atoms in one atomic layer are investigated. The total-energy calculations are performed within the density functional theory in the local density approximation. The electron-electron interaction is described by the Ceperley-Alder functional. The interaction of the electrons with the atomic cores is treated by nonnormconserving *ab initio* ultrasoft pseudopotentials [15]. An energy cutoff of 130 eV is used. Explicitly we use the VASP code [16]. In the bulk case, our calculation yields a cubic lattice constant of $a_0 = 5.398$ Å and an indirect fundamental energy gap of $E_g = 0.46$ eV.

The surfaces are modeled by repeated slabs. Each 16 × 2 slab consists of seven atomic layers and nine layers of vacuum. The bottom sides of the slabs are passivated by hydrogen atoms and kept frozen during the surface optimization. The topmost five layers of each slab are allowed to relax. Two **k** points are used in the irreducible part of the Brillouin zone. The surface geometry is determined allowing to relax the atomic positions until the Hellmann-Feynman forces are less than 10 meV/Å. The eigenvalues and eigenfunctions of the Kohn-Sham equation [17] are used to calculate the STM images within the Tersoff-Hamann approach [18] assuming a constant-height mode.

In order to get an idea about the convergence of the total-energy and force calculations using the 16 × 2 oblique Bravais lattice, we have first studied the ideal, relaxed Si(110) surface. The bond-rotation relaxation with all chains buckled in one direction gives rise to an energy gain of 0.44 eV per 1 × 1 unit cell (see Table I).

This is the same value as computed using the 1×1 rectangular Bravais lattice [12].

It is extremely important to understand the reason for the trenches observed within STM. A structure with two terraces and two steps in a 16×2 unit cell is prepared by removing one half of the first-layer atoms along the $[\bar{1}12]$ direction. However, a simple bond rotation relaxation of the atoms on both terraces as in the 1×1 case yields an energy gain smaller than the value of 0.44 eV/(1×1) cell for the flat, relaxed Si(110)-(1×1) surface. A more intelligent adaption of the steps parallel to $[\bar{1}12]$ and the zigzag chains parallel to $[\bar{1}10]$ is needed. One idea is presented in Fig. 1(a). It is based on the result that a 1×2 reconstruction with chains buckled in opposite directions lowers the surface energy more than the ideal 1×1 case [12]. As a result of the chain buckling in opposite directions different distances of the chains parallel to [001] occur on both terraces. These distances between chains with raised and lowered atoms are denoted in Fig. 1(a) as "upper" and "lower." There are also lateral displacements of the chain atoms which nearly conserve the bond lengths. Buckled atoms allow two basically different bonding configurations between chain atoms of the upper and lower terraces across a step. After the formation of the trench each edge atom on the uppermost terrace possesses two dangling bonds (DBs). One of these DBs may be rebonded with a DB of an atom from the lower terrace if their distance is not too large. According to Fig. 1(a) the lowered atom of a chain of the upper terrace is more preferred to continue a chain on the lower terrace. The described step structure is indeed energetically favorable. The surface energy of the system with oppositely buckled chains on the terraces and rebonded step atoms is lower in energy by 20 meV/(1×1) unit cell (see Table I) compared with the surface without steps.

In order to explain the fine structure of the stripes observed in the STM images of the Si(110)-(16×2) surface [1,4,5], one has to deal with larger reconstruction elements or building blocks consisting of several atoms. The restriction to chains with only up and down atoms is

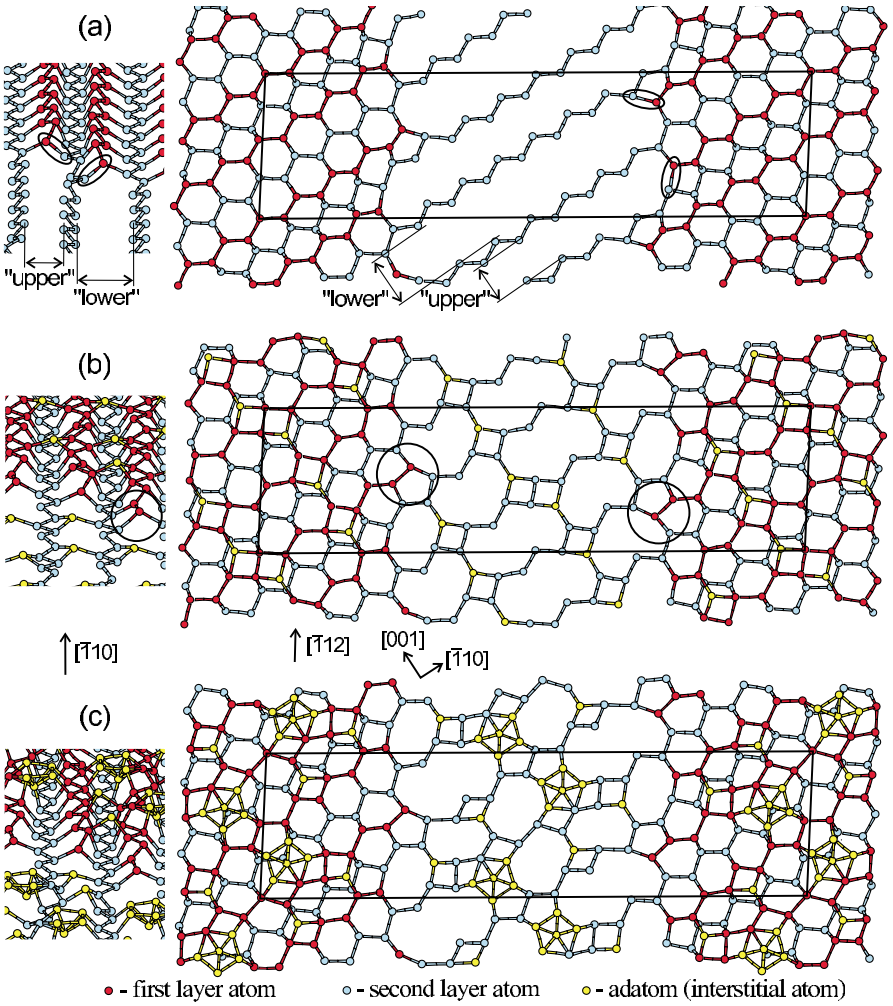

FIG. 1 (color). Top views (right panels) of relaxed atomic structures of Si(110)-(16×2) surfaces: (a) oppositely buckled chain model with steps, (b) adatom model, and (c) adatom-tetramer-interstitial model. Corresponding perspective views (left panels) show parts of the reconstructions along the step. Solid lines indicate a unit cell.

TABLE I. Reconstruction-induced energy gain for different models of the 16×2 reconstruction with respect to the bulk-terminated Si(110) surface.

Reconstruction	ΔE_{surf} [eV/(1 × 1) cell]
chain	0.44
chain on terraces	0.46
adatom	0.47
stretched hexagon	0.18
TI	0.39
ATI	0.49

insufficient. Important parts of such reconstruction elements or building blocks could be adatoms which saturate three dangling bonds and leave one at an adatom itself [12]. We found the most favorable geometry where the adatoms have been arranged almost along the [001] direction as presented in Fig. 1(b). It does not contain the maximum number of adatoms with the consequence of a relatively high number of rest atoms on each terrace. Electron transfer between adatoms to rest atoms and, hence, an accompanying energy gain, are more likely. The rebonded steps are modified by an attachment of adatoms which partly keep their character. In particular, as marked by circles in Fig. 1(b), rebonded step atoms can be considered as natural continuations of the preferable adatom arrangements along the [001] direction on the lower terrace. With the six adatoms on each terrace one counts a total number of 36 DBs. However, the surface energy is drastically lowered with respect to a rather complete coverage with adatoms. The energy gain is larger by 80 (10) meV/(1 × 1) cell compared with the other adatom model (the terraces with oppositely buckled chains). Three reasons may be responsible for the substantial energy gain: the favorable arrangement of the adatoms, the electron transfer between adatoms and rest atoms, and the modified step structure.

In order to model the stripes in the 16×2 reconstruction, an additional degree of freedom may be discussed due to the possibility of atom removal or even missing rows of atoms [5,8]. One possible realization was suggested by the filled-state STM images with only six protrusions per unit cell on each terrace. According to Packard and Dow [5], the corresponding basic building block consists of missing rows of atoms along $[\bar{1}10]$ and adatoms (not shown in Fig. 1). However, such a geometry results in the highest surface energy for the geometries under consideration. Locally the adatom distribution is rather similar, as in the $c(2 \times 2)$ adatom configuration, which was found recently to be rather unfavorable [12]. Furthermore, generation of missing rows by removal of atoms leaves dangling bonds in unfavorable configurations.

On the Si(110)-(16×2) surface one may expect the occurrence of qualitatively similar reconstruction elements as in the case of the Si(113) surfaces [19]. There are tetramer and interstitial atoms, the combination of which has been shown to give rise to pentagons [12]. In the case of Si(110) surfaces, tetramers are formed by four adatoms. Their origin is different from those on Si(113) surfaces which are formed by rebonding of already existing atoms. We only found metastable structures with pure tetramers with small energy gains. However, the situation changes significantly in the presence of interstitials. There is a chance that tetramer-interstitial (TI) pairs explain the "pairs of pentagons" observed in empty-state STM images as suggested in the model of An *et al.* [4]. To model the complete geometry of the 16×2 reconstruction one has also to adapt the step configuration discussed in Figs. 1(a) and 1(b). The stripes on the lower and higher terraces are described by pairs of pentagon-shaped reconstruction elements. Each element consists of a tetramer of four adatoms which has captured an interstitial atom. Similar to what we found in the Si(113) case [20] the capture induces a certain bonding to one atom in an underlying chain. The connecting line of the chain atom and the interstitial in the resulting centered pentamer is almost parallel to the [001] direction. The calculations show that TI reconstruction elements (Table I) are remarkably stabilized in the presence of additional adatoms, the number of which is however not well fixed. The adsorption of two additional atoms for each pentamer gives the largest energy gain as in the case of Si(110)-(3×2) reconstruction [12]. The resulting 16×2 adatom-tetramer-interstitial (ATI) geometry is represented in Fig. 1(c). Indeed, the surface energy is lowered substantially by 100 meV/(1 × 1) cell with respect to the case without additional adatoms. This large energy gain is mainly due to the strong *s* character of the DBs situated at the adatoms which induces an electron transfer from the pentamers resulting in lone pairs of electrons. Instead of the eight adatoms per 16×2 unit cell we have also studied geometries with 12 or four adatoms. The accompanying energy gains were only 10–15 meV/(1 × 1) cell lower than for the eight-adatom case. Therefore, we conclude that probably the number of adatoms per pentamer may vary on real surfaces at room temperature and above.

The long-range 16×2 reconstruction is governed by an interplay of the two steps running along $[\bar{1}12]$ and the structural elements forming the stripes. The formation of trenches and the rebonding across the steps reduce the number of dangling bonds from 64 to 60. The arrangement of two tetramers with interstitial atoms and an appropriate number of accompanying adatoms in a unit cell between two steps further lowers the total energy. These elements need a certain distance to accommodate the induced strain field and to allow for an arrangement of adatoms along [001] over both terraces. This results in an optimal step distance or terrace width of about $4a_0/\sqrt{3} \approx 12.5$ Å and, hence, to the 16×2 reconstruction.

In any case, the ATI reconstruction in Fig. 1(c) yields the lowest surface energy for models of the Si(110)-(16×2) surface with trenches and terraces. However, the corresponding energy gain of 0.49 eV/

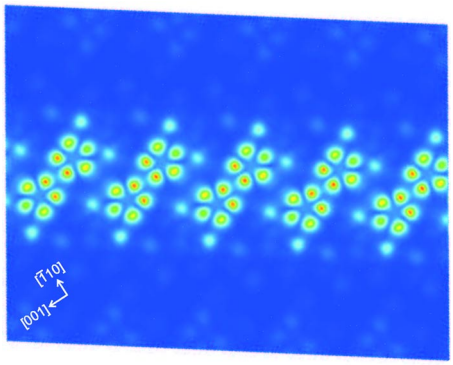

FIG. 2 (color online). Simulated STM image of empty states of the Si(110)-(16 × 2) ATI reconstruction for bias voltage of 1 eV with respect to the theoretical Fermi level. Five unit cells translated along the [1̄12] direction are represented.

(1 × 1) cell is still somewhat smaller than the gain of 0.54 eV/(1 × 1) cell [12] obtained for the ATI reconstruction of the Si(110)-(3 × 2) surface. Either the 16 × 2 reconstruction does not represent the equilibrium surface phase or a modified reconstruction model is needed. Kinetic barriers and substrate doping may play a role during surface preparation. Usually the observation of the 16 × 2 phase is only allowed for less doped substrates. Such a preparation dependence is known for the Si(111) surface with the 2 × 1 reconstruction after low-temperature cleavage and the 7 × 7 translational symmetry after annealing [21]. Finally, a completely new, more complex reconstruction model cannot be excluded.

Besides the surface energy, other important arguments for the validity of a reconstruction model follow from accompanying STM images. An empty-state image is presented in Fig. 2 for the 16 × 2 ATI reconstruction. Because of the constant-height mode used in the simulation, mainly spots from upper terraces are visible. The figure shows that the stripes observed in the measured STM images can really be simulated within an ATI reconstruction. The stripes parallel to the [1̄12] direction consist of pairs of extended reconstruction elements arranged in zigzag form. They are based on pentamers and accompanied by an additional pair of adatoms. The interstitial atoms captured by the pentamers (or original tetramers) are not seen. Each element in the empty-state image consists of nearly five spots and directly represents a pentagon. Therefore, important features found experimentally can be reproduced but not all. This particularly holds for the zigzag character of the stripes. Comparing with the analysis of An *et al.* , the fine structure of the pairs seems to be somewhat interchanged in the measured and calculated spot distributions. However, other experimental STM observations [5] found different structures.

In conclusion, for the first time we have performed *ab initio* calculations for the Si(110) surface using the observed 16 × 2 translational symmetry. Its unit cells nominally contain 64 atoms in each bulklike atomic layer. We have shown that steps leading to trenches and upper terraces as well as lower terraces are important reconstruction elements. An appropriate rebonding of the step atoms stabilizes the Si(110)-(16 × 2) surface. We found the preference of an adatom-tetramer-interstitial model, where together with an interstitial atom, four adatoms form a pentamer that should be combined with a varying number of one to three adatoms. Obviously, such pentamers can yield pentagonal shapes of spot arrangements in the STM images. The number of the additional adatoms may be related to the degree of pentamer buckling. Both number of adatoms and pentamer asymmetry will influence the number of spots seen in the STM images of filled and empty states.

We acknowledge financial support from the Deutsche Forschungsgemeinschaft (Project No. Be1346/12-1) and the European Community in the framework of the Research and Training Network NANOPHASE (Contract No. HPRN-CT-2000-00167).

[1] Y. Yamamoto, Phys. Rev. B **50**, 8534 (1994).
[2] H. Ampo, S. Miura, K. Kato, Y. Ohkawa, and A. Tamura, Phys. Rev. B **34**, 2329 (1986).
[3] Y. Yamamoto, T. Sueyoshi, T. Sato, and M. Iwatsuki, Surf. Sci. **466**, 183 (2000).
[4] T. An, M. Yoshimura, I. Ono, and K. Ueda, Phys. Rev. B **61**, 3006 (2000).
[5] W. E. Packard and J. D. Dow, Phys. Rev. B **55**, 15643 (1997).
[6] E. J. Van Loenen, D. Dijkkamp, and A. J. Hoeven, J. Microsc. **152**, 487 (1988).
[7] A. Cricenti, B. Nesterenko, P. Perfetti, and C. Sebenne, J. Vac. Sci. Technol. A **14**, 2448 (1996).
[8] E. G. Keim, H. Wormeester, and A. van Silfhout, J. Vac. Sci. Technol. A **8**, 2747 (1990).
[9] A. I. Shkrebtii, C. M. Bertoni, R. Del Sole, and B. A. Nesterenko, Surf. Sci. **239**, 227 (1990).
[10] M. Menon, N. N. Lathiotakis, and A. N. Andriotis, Phys. Rev. B **56**, 1412 (1997).
[11] N. Takeuchi, Surf. Sci. **494**, 21 (2001).
[12] A. A. Stekolnikov, J. Furthmüller, and F. Bechstedt, Phys. Rev. B **70**, 045305 (2004).
[13] T. Ichikawa, Surf. Sci. **544**, 58 (2003).
[14] Z. Gai, R. G. Zhao, and W. S. Yang, Phys. Rev. B **57**, R6795 (1998).
[15] J. Furthmüller, P. Käckell, F. Bechstedt, and G. Kresse, Phys. Rev. B **61**, 4576 (2000).
[16] G. Kresse and J. Furthmüller, Comput. Mater. Sci. **6**, 15 (1996); Phys. Rev. B **54**, 11169 (1996).
[17] W. Kohn and L. J. Sham, Phys. Rev. **140**, A1133 (1965).
[18] J. Tersoff and D. R. Hamann, Phys. Rev. B **31**, 805 (1985).
[19] J. Dabrowski, H.-J. Müssig, and G. Wolff, Phys. Rev. Lett. **73**, 1660 (1994).
[20] A. A. Stekolnikov, J. Furthmüller, and F. Bechstedt, Phys. Rev. B **67**, 195332 (2003); **68**, 205306 (2003).
[21] F. Bechstedt, *Principles of Surface Physics* (Springer, Berlin 2003).